Analytical Biochemistry 389 (2009) 130–137

Contents lists available at ScienceDirect

Analytical Biochemistry

journal homepage: www.elsevier.com/locate/yabio

Cobalt hydroxide nanoparticles modified glassy carbon electrode as a biosensor for electrooxidation and determination of some amino acids

Mohammad Hasanzadeh [a,b,*], Ghasem Karim-Nezhad [a], Nasrin Shadjou [a,b], Maryam Hajjizadeh [b], Balal Khalilzadeh [c], Lotfali Saghatforoush [a], Mohammad Hossein Abnosi [d], Ali Babaei [c], Sohrab Ershad [e]

[a] Department of Analytical Chemistry, Faculty of Science, Payame Noor University, P.O. Box 58168-45164, khoy, Iran
[b] Department of Chemistry, Faculty of Science, K. N. Toosi University of Technology, Tehran, Iran
[c] Department of Analytical Chemistry, Faculty of Science, Arak University, Arak, Iran
[d] Department of Biochemistry, Faculty of Science, Arak University, Arak, Iran
[e] Department of Chemistry, Payame Noor University, Marand, Iran

ARTICLE INFO

Article history:
Received 5 February 2009
Available online 21 March 2009

Keywords:
Amino acids
Electrocatalysis
Modified electrode
Alkaline media

ABSTRACT

The electrochemical behavior of some amino acids was investigated on cobalt hydroxide nanoparticles modified glassy carbon (CHM–GC) electrode in alkaline solution. The process of oxidation and its kinetics were established by using cyclic voltammetry, chronoamperometry techniques, and steady-state polarization measurements. The results revealed that cobalt hydroxide promotes the rate of oxidation by increasing the peak current, so these bimolecular reactions are oxidized at lower potentials. Cyclic voltammograms and chronoamperometry indicate a catalytic EC′ mechanism to be operative with electrogeneration of Co(IV) as the electrochemical process. Also, the process is diffusion controlled and the current–time responses follow Cottrellian behavior. This result was confirmed by steady-state measurements. The rate constants of the catalytic oxidation of amino acids and the electron transfer coefficients are reported.

The chemical modification of electrodes with a suitable reagent has been widely used for analytical applications. The resulting electrodes were designed to provide desired selective sites toward the analytes. Chemically modified electrodes (CMEs)[1] have played an important role in the studies of electrocatalysis [1–4], electron transfer kinetics [5,6], membrane barriers [7,8], electroorganic synthesis [9], and the like. One of the most important electrode modification techniques has involved the formation of an electrocatalytic system in which a redox species capable of undergoing a rapid and reversible electrode reaction is incorporated onto the electrode surface. These electrodes reduce the overpotential required for either oxidation or reduction of compounds. Many mixed valent compounds such as oxides, complexes, or alloys of copper [10–12], cobalt [13–15], and ruthenium [16–18] have shown electrocatalytic properties.

Immobilized cobalt ion-based materials, which can in principle flip-flop between various valence states under the effect of external electric field, on the one hand, and the potential reducing agent, on the other, are of particular interest. The preparation, characterization, and electrochemistry of cobalt hydroxide (oxide)-containing films have been studied extensively in alkaline medium [19,20]. Various methods of preparation, ranging from spray pyrolysis [21], sonication [22], and sputtering [23] to electrodepositing from aqueous solutions containing complexion agents and at various pH values, have been considered [24–27]. In particular, substantial efforts have been dedicated to the development of biosensors using cobalt hydroxide nanoparticles modified (CHM) electrode. Meanwhile, little attention has been paid to the electrocatalytic activities of cobalt hydroxide (oxide) modified electrodes in the electrooxidation of amino acids.

The oxidation and adsorption behaviors of amino acids on electrode surfaces are relevant to the interfacial behaviors of proteins (biological molecules) and also to the medical and industrial problems associated with the adsorption of the proteins on the surfaces [28–30]. The problem with the application of electrochemical methods for amino acid and protein analysis is the lack of electrochemically active groups in most of these compounds. Thus, a derivatization procedure must be used prior to determination of amino acids. Two approaches are adopted. The first approach is

* Corresponding author. Address: Department of Analytical Chemistry, Faculty of Science, Payame Noor University, P.O. Box 58168, Khoy 45164, Iran. Fax: +98 461 2332556.
E-mail address: mhmmd_hasanzadeh@yahoo.com (M. Hasanzadeh).

[1] *Abbreviations used:* CME, chemically modified electrode; CHM, cobalt hydroxide nanoparticles-modified; SCE, saturated calomel electrode; Pt, Platinum; GC, glassy carbon; CV, cyclic voltammogram; DPV, differential pulse voltammetry; LOD, limit of detection; LOQ, limit of quantitation; RSD, relative standard deviation.

0003-2697/$ - see front matter © 2009 Elsevier Inc. All rights reserved.
doi:10.1016/j.ab.2009.03.024

to derivate the analyte with an electrochemically active group prior to determination. The second approach is to generate in situ chemical reactions on electrode surfaces to produce electrochemically active products for detection [31].

The current study, a continuation of our studies on biological molecules [31–36], was an attempt to develop and apply the modified electrodes that were aimed at inspecting the kinetics of electrochemical processes [37–40]. Amino acid analysis has an extensive impact on public health. Electrochemical techniques have been used for the determination of a wide range of amino acids [41–45]. The findings of this study show the results of the anodic oxidation of amino acids on a glassy carbon surface where catalytically active cobalt hydroxide is deposited. The study was carried out with 100 mM sodium hydroxide solution. Therefore, it is essential to develop simple and rapid methods for electrooxidation of these biological molecules in routine analysis.

Materials and methods

Electrochemical experiments were performed at 22 ± 3 °C in a conventional three-electrode cell using a potentiostat/galvanostat AUTOLAB system with PGSTAT12 boards (Eco Chemie, Utrecht, Netherlands). The system was run on a PC using GPES 4.9 software. Doubly distilled water was used to prepare the solutions. A saturated calomel electrode (SCE) and a platinum (Pt) wire were used as the reference electrode and counter electrode, respectively. Films of cobalt hydroxide were formed on the glassy carbon (GC) electrode with a surface area of 0.125 cm^2 by the method reported previously by Casella [26]. The modified electrodes reproduced by cycling the potential of the working electrode in the range of −250 to 750 mV (vs. SCE) at a scan rate of 100 mV s^{-1} for 70 cycles. The surface concentration of cobalt hydroxide was controlled by the number of cycles applied to the deposition process and was electrochemically evaluated in 100 mM NaOH solution. Prior to the modification, the GC electrode was polished with a 0.05-μm alumina suspension on a polishing microcloth and rinsed thoroughly with doubly distilled water.

Results and discussion

Fig. 1A presents 75 consecutive cyclic voltammograms (CVs) of a GC electrode in the presence of 100 mM Na_2CO_3 + 40 mM NaK tartrate + 4 mM $CoCl_2$ at pH 11.6 recorded at a potential sweep rate of 100 mV s^{-1}. The CVs are similar to those reported in the literature [26,27]. Fig. 1B shows a CV of the CHM–GC electrode in 100 mM NaOH solution in the range of −200 to 690 mV recorded at a potential sweep rate of 100/mV s^{-1}. It consists of anodic peaks located at 225 and 550 mV/SCE that are attributed to Co(II)/Co(III) and Co(III)/Co(IV) redox transition associated with different cobalt oxide species on the electrode surface [30,46]. The cathodic peaks at 186 and 522 mV correspond to the reduction of various cobalt oxide species formed during the anodic sweep.

Fig. 2A presents typical CVs of a CHM–GC electrode in 100 mM NaOH solution at various potential sweep rates from 2 to 150 mV s^{-1}. The peak currents are proportional to sweep rates in the range of 2 to 75 mV s^{-1}, as shown in Fig. 2B and C, pointing to the electrochemical activity of the surface redox couple. From the slope of this lines and using

$$I_p = \left(\frac{n^2F^2}{4RT}\right)\nu A\Gamma^*, \quad (1)$$

where Γ^* is the surface coverage of the redox species and ν is the potential sweep rate [47,48]. Taking the average of both cathodic and anodic results, Γ^* values of approximately 1.98×10^9 mol cm^{-2} have been derived. In the high ranges of sweep rates, this dependency is of the square root form, as shown in Fig. 2D and E, signifying the dominance of the diffusion-controlled processes.

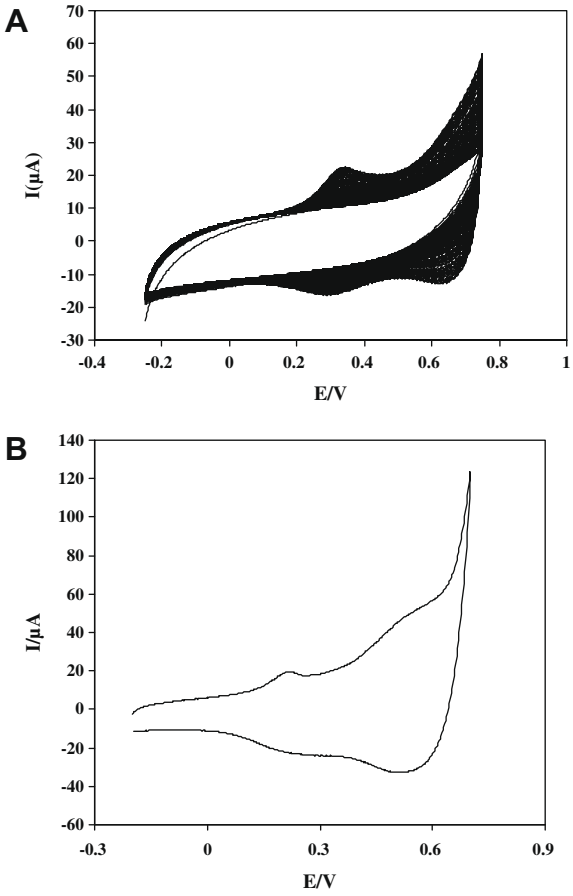

Fig. 1. (A) CVs for 4 mM $CoCl_2$ + 40 mM Na–K tartrate + 100 mM Na_2CO_3 using a GC electrode. The potential was scanned continuously at 100 mV s^{-1} between −250 and 750 mV. (B) CVs of a CHM–GC in 100 mM NaOH solution in the range of –200 to 690 mV/SCE with a sweep rate of 100 mV s^{-1}.

Fig. 3A illustrates CVs of 0.8 mM Cys using the CHM–GC electrode recorded at different potential sweep rates. Fig. 3B indicates that anodic peak currents increased linearly with the square root of the potential sweep rate, indicating a mass transfer-controlling process of oxidation via diffusion. In addition, the value of the electron transfer coefficient for the reaction can be obtained from the following equation [47]:

$$Ep = \left(\frac{RT}{2\alpha F}\right)\ln\nu + \text{constant}. \quad (2)$$

This is valid for a totally irreversible diffusion-controlled process. Using the dependency of anodic peak potential on the Neperian logarithm of the potential sweep rate (Fig. 3C), the value of the electron transfer coefficient was obtained as 0.61. The Tafel slope is 40.61. On the basis of the slopes of the linear dependency of the anodic peak currents on the square root of the potential sweep rates (Fig. 3B) and the Randles–Sevcik equation [47],

$$I_p = (2.99 \times 10^5)\alpha^{1/2}n^{3/2}AC^*D^{1/2}\nu^{1/2}, \quad (3)$$

where I_p is the peak current, A is the electrode surface area, C^* is the bulk concentration of amino acids, and D is the diffusion coefficient. The diffusion coefficient for Cys was calculated to be 9.05×10^{-5} cm^2 s^{-1}.

Fig. 4A presents the CVs of CHM–GC in both the absence and presence of 5 mM Cys in 100 mM NaOH solution. At the CHM–GC electrode, oxidation of Cys resulted in a typical electrocatalytic

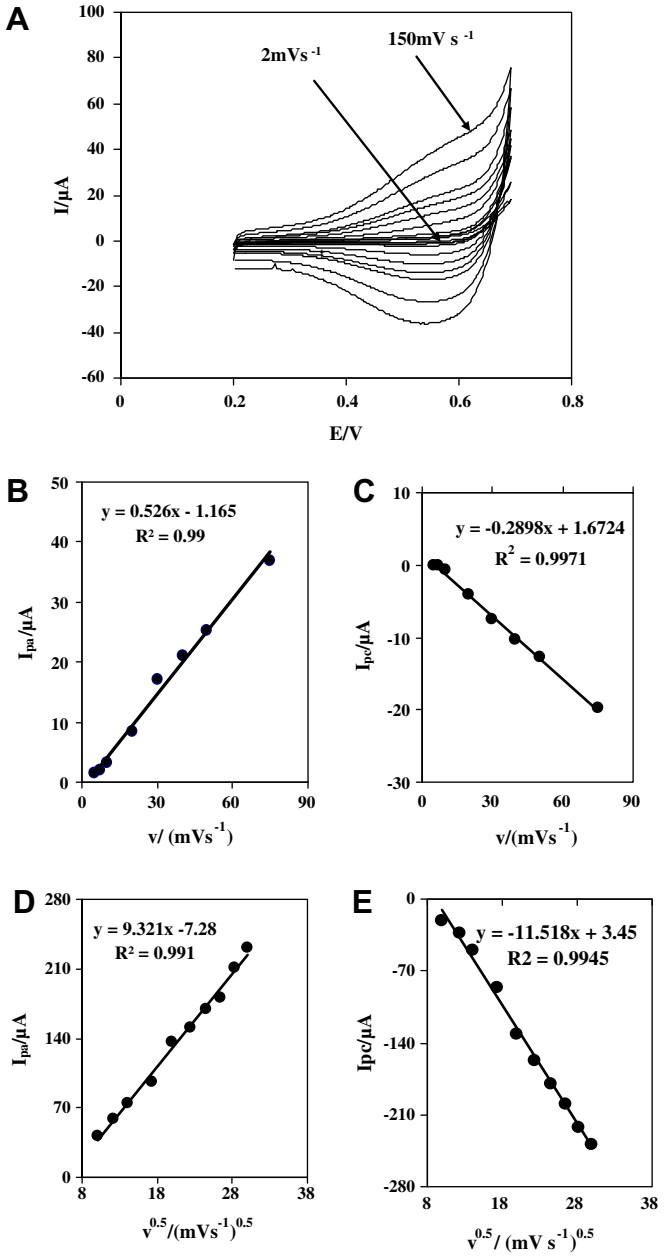

Fig. 2. Typical CVs of a CHM–GC electrode in 100 mM NaOH at the potential sweep rates of 2, 5, 7, 10, 20, 30, 40, 50, 75, 100, and 150 mV s^{-1} (A) the dependency of anodic (B) and cathodic (C) peak currents to the sweep rate at lower values (2–75 mV s^{-1}), and the proportionality of anodic (D) and cathodic (E) peak currents to the square roots of sweep rate at higher values (100–900 mV s^{-1}).

response. In the presence of Cys, it was observed that the anodic current and the associated anodic charge increased dramatically, whereas the cathodic current and the corresponding charge decreased. In the presence of Cys, the i_{pa}/i_{pc} ratio was 71.36; in the absence of Cys, this ratio was decreased to 34.21. This result indicates that Cys is oxidized by active Co(IV) moiety through a cyclic mediation redox process. Cobalt species are immobilized on the electrode surface, and the one with a higher valence oxidizes to Co(IV) via a chemical reaction followed by the generation of low-valence cobalt (Co(III) species). Along this line, the high-valence oxide is regenerated through the external electrical circuit. Accordingly, Cys is oxidized via an EC′ mechanism. Finally, we noticed that the peak current values exhibited a linear dependence on the concentration of Cys, suggesting the utility of the modified electrodes for analytical applications.

Fig. 4B shows that on increasing the concentration of Cys, its irreversible oxidation develops in the region of the electrochemical formation of Co(IV). Thus, it is likely that the electrogenerated Co(IV) species is the active moiety that efficiently speeds up the oxidation of amino acids. Any increase in the concentration of Cys causes a proportional and nearly linear enhancement of the anodic wave. It is worthwhile to emphasize that the anodic formation of Co(IV) seems to be an irreversible process. Also, plotting the current function (peak current divided by the square root of the potential sweep rate) against the square root of the potential sweep rate (Fig. 4C) revealed a negative slope, confirming the electrocatalytic nature of the process.

Similar CVs were recorded for Val, l-Phe, l-Arg, Gly, Ser, Tyr, Cys, and l-Trp. The values of a and b (Tafel slope) were obtained for these amino acids according to this method and are reported in Table 1.

The redox transition of cobalt species present in the film is

$$\mathrm{CO(III)} \underset{k-1}{\overset{K_1}{\rightleftharpoons}} \mathrm{CO(IV)} + e, \tag{4}$$

and Cys is oxidized on the modified surface via the following reaction:

$$\mathrm{CO(IV)} + \text{cysteine} \overset{k_2(E)}{\rightarrow} \text{intermediate} + \mathrm{CO(III)}, \tag{5}$$

where the intermediate is further oxidized to the product through a similar electrooxidation process:

$$\mathrm{CO(IV)} + \text{intermediate} \overset{k_3(E)}{\rightarrow} \text{product} + \mathrm{CO(III)}. \tag{6}$$

The oxidation process CHM–GC electrode exhibited similar electrocatalytic responses for the amino acids Val, l-Phe, Cys, l-Arg, Gly, Ser, Tyr, and l-Trp, thereby exhibiting its capability for selective oxidation of amino acids.

Chronoamperometry and cyclic voltammetry have been employed for the investigation of the processes occurring via an E_rC_i mechanism [47]. Double step chronoamperograms were recorded by setting the working electrode potentials to desired values and were used to measure the catalytic rate constant on the modified surface. Fig. 5A shows double step chronoamperograms for the modified electrode in the absence and presence of Cys over a concentration range of 1–25 mM. The applied potential steps were 220 and 600 mV, respectively. The plot of net current versus $t^{-0.5}$, which was obtained by removing the background current by the point-by-point subtraction method, gives a straight line (Fig. 5B). This indicates that the transient current must be controlled by a diffusion process. The transient current is due to catalytic oxidation of Cys that increases as the Cys concentration is raised. No significant cathodic current was observed when the electrolysis potential was stepped to 220 mV/SCE, indicating the irreversible nature of the oxidation of amino acids by using the slopes of these lines. We can obtain the diffusion coefficients of the amino acids according to the Cottrell equation [47]:

$$I = nFAD^{1/2}C^*\pi^{-1/2}t^{-1/2}, \tag{7}$$

where D is the diffusion coefficient and C^* is the bulk concentration. The mean value of the diffusion coefficients of Cys was founded to be $(8.9 \pm 0.02) \times 10^{-5}$ cm^2 s^{-1}. These values are in agreement with those obtained using cyclic voltammetry (Fig. 4).

The rate constants of the reactions of Cys and the ensuing intermediates with the redox sites of the CHM–GC electrode can be derived from the chronoamperograms according to Eq. (8) [47]:

$$\frac{I_{\mathrm{catal}}}{I_{\mathrm{d}}} = \lambda^{1/2}\left[\pi^{1/2}erf(\lambda^{1/2}) + \frac{\exp(-\lambda)}{\lambda^{1/2}}\right], \tag{8}$$

where I_{catal} is the catalytic current in the presence of Cys, I_d is the limiting current in the absence of Cys, and $\lambda = kCt$ (where k, C, and

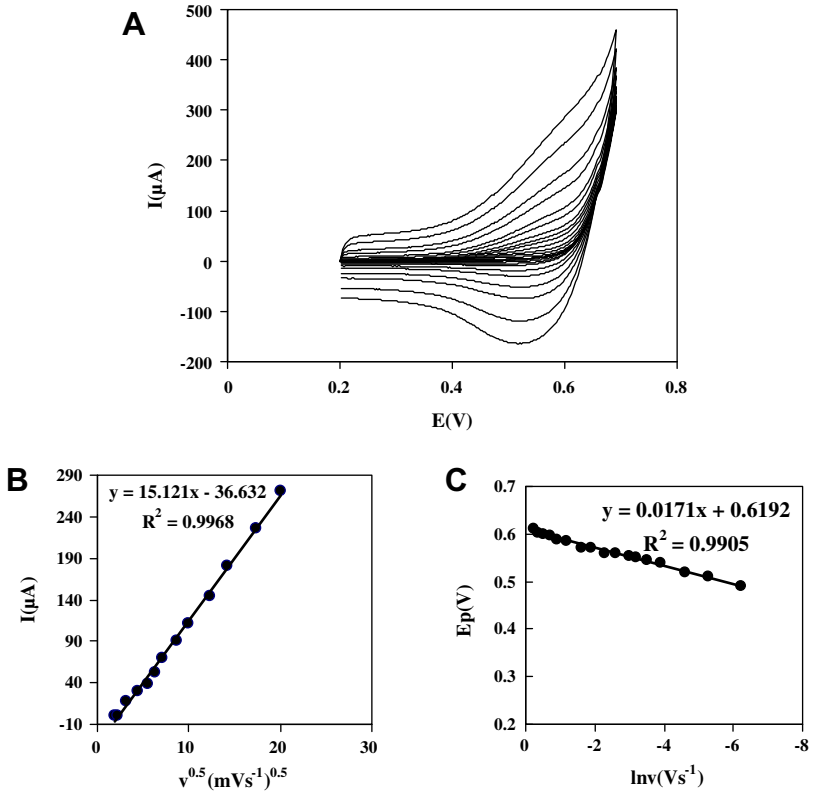

Fig. 3. (A) CVs of the CHM–GC electrode in 100 mM NaOH solution in the presence of 0.8 mM Cys at various potential sweep rates of 2, 5, 10, 20, 30, 40, 50, 75, 100, 150, 200, 300, and 400 mV s^{-1}. (B) Dependence of anodic peak current during the forward sweep on the square roots of potential sweep rate. (C) Dependence of peak potential on log ν for the oxidation of Cys at CHM–GC electrode obtained from the data of panel A.

t are the catalytic rate constant, bulk concentration of Cys, and elapsed time, respectively) is the argument of the error function. For $\lambda > 1.5$, *erf* $(\lambda^{1/2})$ nearly equals unity and Eq. (8) reduces to

$$\frac{I_{\text{catal}}}{I_{\text{d}}} = \lambda^{1/2}\pi^{1/2} = \pi^{1/2}(kCt)^{1/2}. \tag{9}$$

From the slope of the $I_{\text{catal}}/I_{\text{d}}$ plot, the value of k at a given concentration of Cys can be derived. The mean value of k in the concentration range of 1–25 mM Cys was found to be $(3.62 \pm 0.03) \times 10^5$ cm^3 mol^{-1} s^{-1}. It should be pointed out that k is either k_2 or k_3, whichever is smaller. Similar chronoamperograms were collected for Val, Phe, Cys, Arg, Gly, Ser, Tyr, and Trp. The values of D and k obtained according to the method described above for these bimolecular reactions are reported in Table 1.

The rate laws for the Reactions (4) and (5) have the forms of

$$\nu_1 = k_1\Gamma\theta_{\text{III}} - k_{-1}\Gamma\theta_{\text{IV}} \tag{10}$$

$$\nu_2 = k_2\Gamma\theta_{\text{IV}}C_{\text{m}}, \tag{11}$$

where Γ is the total number of adsorption sites per unit area of the electrode surface, θ represents the fractional surface coverages of different cobalt valence states, and C_{m} is the bulk concentration of Cys. With only the 3 and 4 valence states of cobalt prevailing, one has

$$\theta_{\text{III}} + \theta_{\text{IV}} = 1. \tag{12}$$

The rates of changes of their surface coverages, as well as those of the intermediate compounds, are

$$\frac{d\theta_{\text{III}}}{dt} = -\frac{d\theta_{\text{IV}}}{dt} = -k_1\theta_{\text{III}} + k_{-1}\theta_{\text{IV}} + k_2\theta_{\text{IV}}C_m + k_3\theta_{\text{IV}}C_{\text{i}} \tag{13}$$

$$\frac{dc_{\text{i}}}{dt} = k_2\theta_{\text{IV}}C_{\text{m}} - k_3\theta_{\text{IV}}C_{\text{i}}, \tag{14}$$

where C_{i} is the concentration of the intermediate. Assuming that the steady state dominates,

$$\frac{d\theta_{\text{III}}}{dt} = -\frac{d\theta_{\text{IV}}}{dt} = 0 \tag{15}$$

$$\frac{dC_{\text{i}}}{dt} = 0. \tag{16}$$

One arrives at the values if the coverages

$$\theta_{\text{III}} = \left(\frac{k_{-1} + 2k_2C_{\text{m}}}{k_1 + k_{-1} + 2k_2C_{\text{m}}}\right) \tag{17}$$

$$\theta_{\text{IV}} = \left(\frac{k_1}{k_1 + k_{-1} + 2k_2C_{\text{m}}}\right) \tag{18}$$

and subsequently

$$\nu_1 = \left(\frac{2k_1\Gamma k_2C_{\text{m}}}{k_1 + k_{-1} + 2k_2C_{\text{m}}}\right). \tag{19}$$

On the basis of this rate equation, the faradic current will be

$$i_{\text{f}} = \left(\frac{2FAk_1\Gamma k_2C_{\text{m}}}{k_1 + k_{-1} + 2k_2C_{\text{m}}}\right). \tag{20}$$

where A is the surface area of the electrode and the rate constants k_1 and k_{-1} are obviously potential dependent and are of the forms

$$k_1(E) = k_1^0 \exp\left[\frac{\alpha nFE}{RT}\right] \tag{21}$$

$$k_{-1}(E) = k_{-1}^0 \exp\left[\frac{(\alpha - 1)nFE}{RT}\right], \tag{22}$$

where k_{-1}^0 and k_1^0 are the chemical rate constants measured at E/SCE = 0, with α being the anodic transfer coefficient and other parameters having their usual meanings. Eq. (20) is well suited for

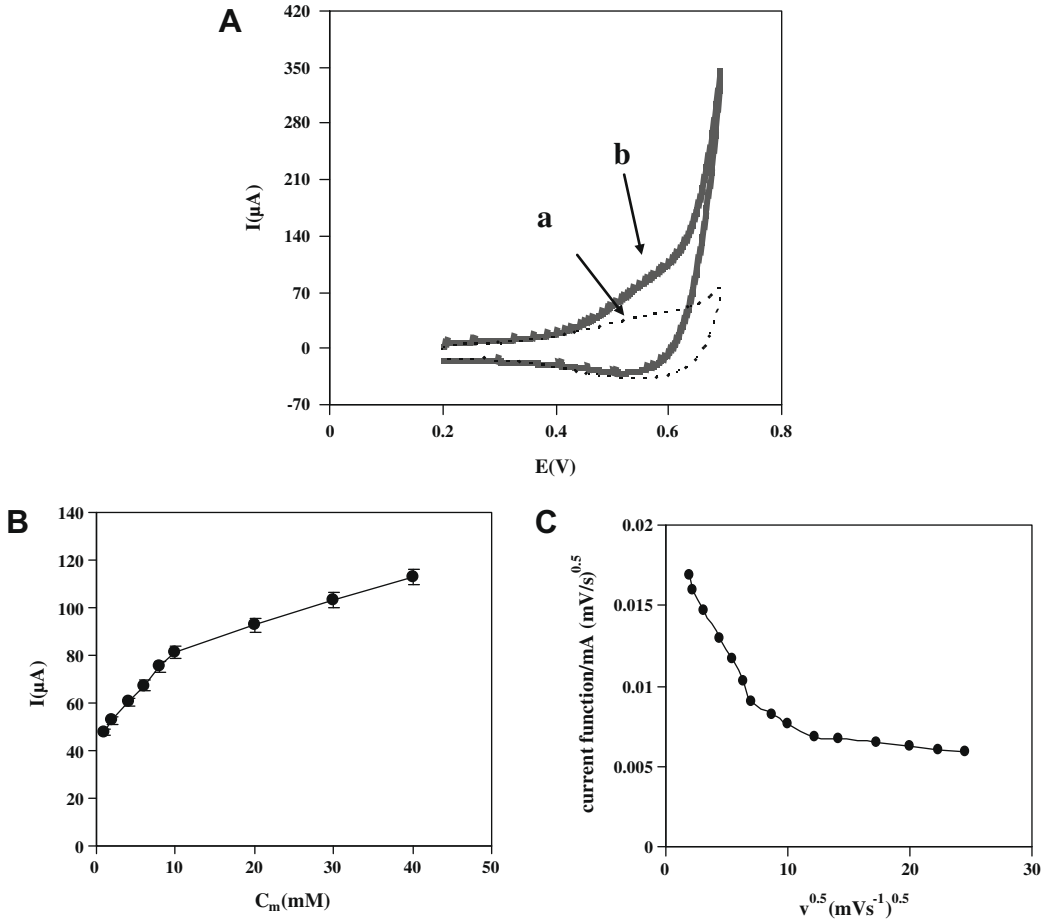

Fig. 4. (A) CVs of the CHM–GC electrode in 100 mM NaOH solution in the absence (a) and presence (b) of 5 mM Cys. The potential sweep rate was 100 mV s^{-1}. (B) Dependency of the anodic peak current electrooxidation on Cys concentrations. (C) current function vs. $v^{0.5}$ for 100 mM NaOH solution in the presence of 8 mM Cys.

Table 1
Values of diffusion coefficients (D) and electrocatalytic reaction rate constants (k) obtained from chronoamperometry and $k_2\Gamma$, $k_1^0\Gamma$, α, and b (Tafel slope) obtained from polarization curves.

b	α	$k_1^0\Gamma$ (mol s^{-1} cm^{-2})	$k_2\Gamma$ (cm s^{-1})	k (cm^3 mol^{-1} s^{-1})	D (cm^2 s^{-1})	Amino acid
55.05 ± 0.03	0.45 ± 0.03	5.21×10^{-9}	9.39×10^{-10}	$(3.62 \pm 0.03) \times 10^5$	$(8.9 \pm 0.02) \times 10^{-5}$	Cys
49.55 ± 0.03	0.50 ± 0.02	8.42×10^{-8}	4.31×10^{-9}	$(1.53 \pm 0.02) \times 10^6$	$(3.2 \pm 0.04) \times 10^{-5}$	Gly
40.61 ± 0.03	0.61 ± 0.03	9.11×10^{-7}	1.34×10^{-8}	$(3.44 \pm 0.02) \times 10^5$	$(8.4 \pm 0.02) \times 10^{-6}$	Tyr
65.12 ± 0.03	0.45 ± 0.03	1.81×10^{-9}	8.30×10^{-10}	$(2.22 \pm 0.03) \times 10^6$	$(1.7 \pm 0.03) \times 10^{-5}$	Ser
56.48 ± 0.03	0.44 ± 0.02	4.81×10^{-8}	5.88×10^{-10}	$(1.02 \pm 0.04) \times 10^6$	$(4.4 \pm 0.03) \times 10^{-6}$	Val
61.93 ± 0.03	0.40 ± 0.04	2.53×10^{-9}	6.64×10^{-11}	$(7.33 \pm 0.02) \times 10^5$	$(6.9 \pm 0.02) \times 10^{-5}$	l-Arg
60.61 ± 0.03	0.41 ± 0.03	1.03×10^{-8}	8.11×10^{-10}	$(2.28 \pm 0.04) \times 10^6$	$(3.0 \pm 0.04) \times 10^{-5}$	l-Phe
41.64 ± 0.03	0.51 ± 0.03	7.49×10^{-7}	1.21×10^{-8}	$(4.26 \pm 0.03) \times 10^5$	$(5.3 \pm 0.02) \times 10^{-5}$	l-Trp

the calculation of rate constants and the validity test of the kinetics and mechanism of the oxidation process.

The pseudo-steady-state polarization curves of the electrooxidation of Cys on the CHM–GC electrode at a number of Cys concentrations are presented in Fig. 6A. The oxidation process was found to begin at nearly 370 mV/SCE and to reach a plateau at 600 mV/SCE, whereas the oxygen evolution started at still higher potentials. In the course of reaction, the coverage of Co(IV) increases and reaches a saturation (steady-state) level and the oxidation current follows accordingly. According to Eq. (23), the plots of the inverse of current against the inverse of Cys concentration should be linear:

$$i_f^{-1} = (FAk_1\Gamma)^{-1} + \left[\frac{k_1 + k_{-1}}{2FAk_1k_2\Gamma}\right] C_m^{-1} \qquad (23)$$

Fig. 6B presents the i^{-1} versus $C_m{}^{-1}$ dependency where straight lines at various potentials have been obtained. Both the intercepts and slopes of the straight lines appearing in this figure were potential dependent. The slopes are plotted against exp($-nFE/RT$) with $n = 1$, and the graph is presented in Fig. 6C. Using this graph along with Eq. (23) reveals that the rate constant of Reaction (5), $k_2\Gamma$, and the ratio of k_{-1}^0/k_1^0 are 9.39×10^{-10} cm s^{-1} and 6.78×10^9, respectively. Fig. 6D presents the variation of the intercepts of the lines in Fig. 6B with the applied potential on a semilog scale.

Using this graph and Eq. (23), the magnitudes of $k_1^0\Gamma$ and the anodic transfer coefficient of 5.21×10^{-9} mol s^{-1} cm^{-2} and 0.45 have been obtained. From the above findings, the value of $k_{-1}^0\Gamma$ was worked out to be 3.41×10^1 mol s^{-1} cm^{-2}. Similar pseudo-steady-state polarization curves were collected for Val, l-Phe, l-Arg, Gly, Ser, Tyr, and l-Trp. The values of $k_2\Gamma$, $k_1^0\Gamma$, α, and b (Tafel slope) ob-

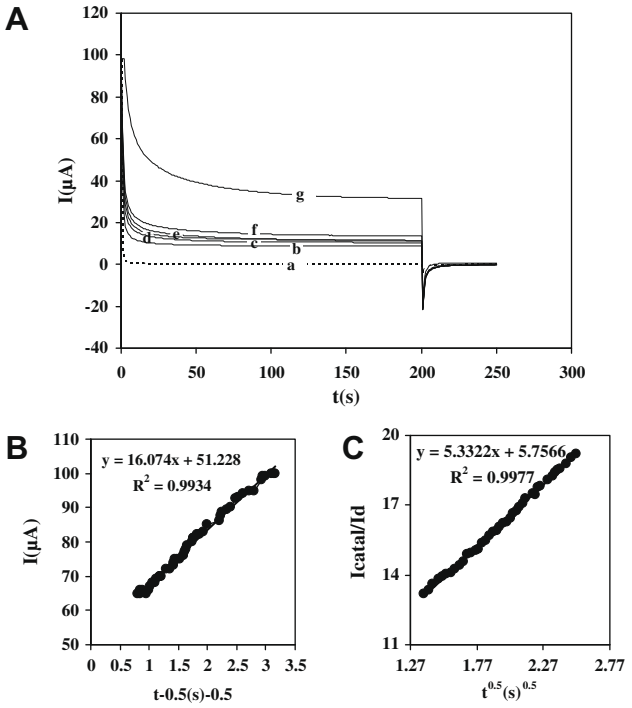

Fig. 5. (A) Double step chronoamperograms of the CHM–GC electrode in the absence of Cys (a) and the presence of 1 mM Cys (b), 4 mM Cys (c), 6 mM Cys (d), 8 mM Cys (e), 10 mM Cys (f), and 25 mM Cys (g) in 100 mM NaOH solution. Potential steps were 600 and 220 mV. (B) Dependency of transient current on $t^{-0.5}$. (C) Dependence of I_{catal}/I_d on $t^{0.5}$ derived from the data of chronoamperograms a to g in panel A.

tained according to the method described above for these amino acids are reported in Table 1.

The calibration curve for Cys concentration in 100 mM NaOH was obtained by differential pulse voltammetry (DPV). Fig. 7A shows typical DPV curves for different concentrations of Cys in alkaline solution. The dependency between peak current and Cys concentration was rectilinear for peak a1 within the range of 0.01 to 15 mM (with a regression equation of $y = 10.048x + 4.384$, $R^2 = 0.9968$, $n = 6$ (Fig. 7B). The limits of detection (LODs) and limits of quantitation (LOQs) of the procedure were calculated according to the 3 SD/m criterion, where SD is the standard deviation of the blank and m is the slope of the calibration curves [49]. The LODs and LOQs were found to be 4.34×10^{-5} M and 8.52×10^{-5} M for peak a1. Precision and accuracy were assessed by performing replicate analyses of Cys samples. The precision of the method was calculated as the relative standard deviation (RSD). The procedure was repeated on the same day on the same solutions at concentrations in the range of the standard series. The intraassay RSD of the proposed method determined on the basis of peak current for 10 replications was 3.4% for peak a1 and showed good repeatability. The analytical parameters obtained for the analyzed samples are summarized in Table 2. Similar DPV curves were collected for Val, l-Phe, l-Arg, Gly, Ser, Tyr, and l-Trp. The values of LODs (μM), LOQs (μM), and linear ranges (μM) obtained according to the method described above for these amino acids are reported in Table 3.

Conclusion

This work has presented the reproducing and usefulness of cobalt hydroxide (oxide) modified glassy carbon electrodes for amino

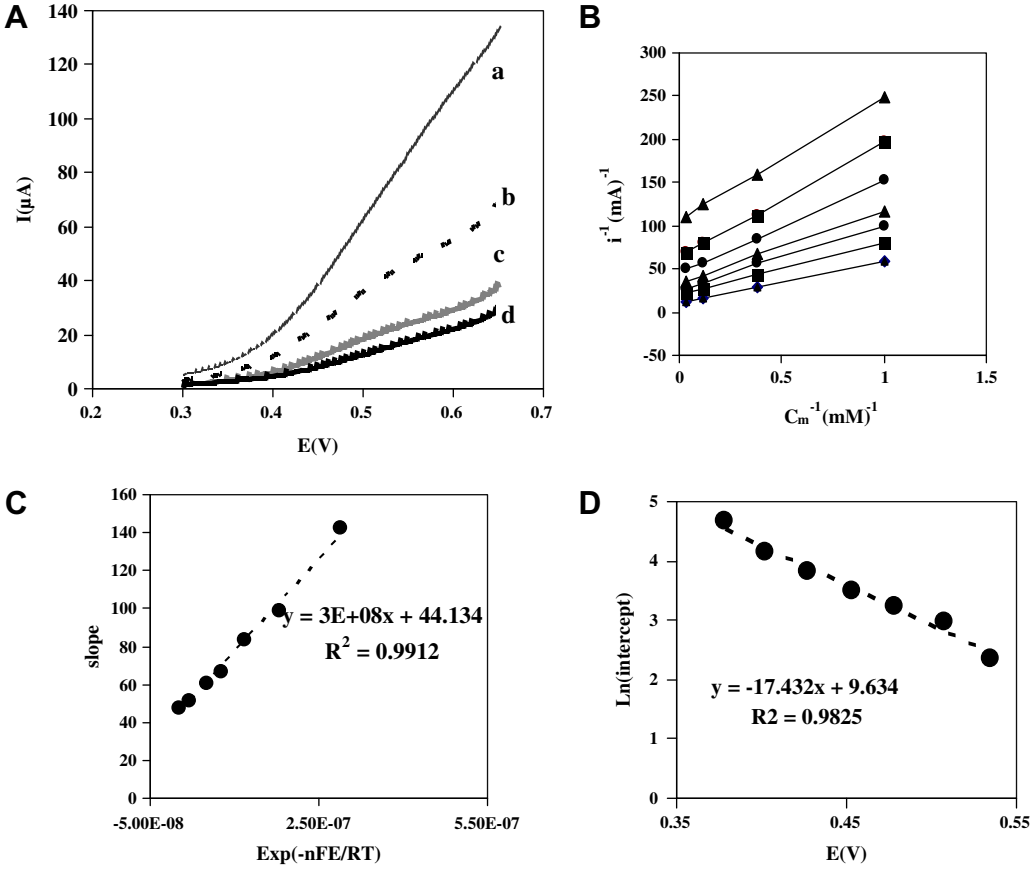

Fig. 6. (A) Typical pseudo-steady state polarization curves of the CHM–GC electrode obtained in 50 mM Cys (a), 25 mM Cys (b), 10 mM Cys (c), and 5 mM Cys (d). (B) Plot of i^{-1} from polorization curves in curve (A) against C_m^{-1} at various potentials: 378, 402, 426, 453, 478, 507 and 534 mV/SCE as curves (a–g). (C) Plot of the slopes (of curves in B) vs. exp(-nFE/RT). (D) Plot of the ln(intercept) (of curves in B) vs. applied potential.

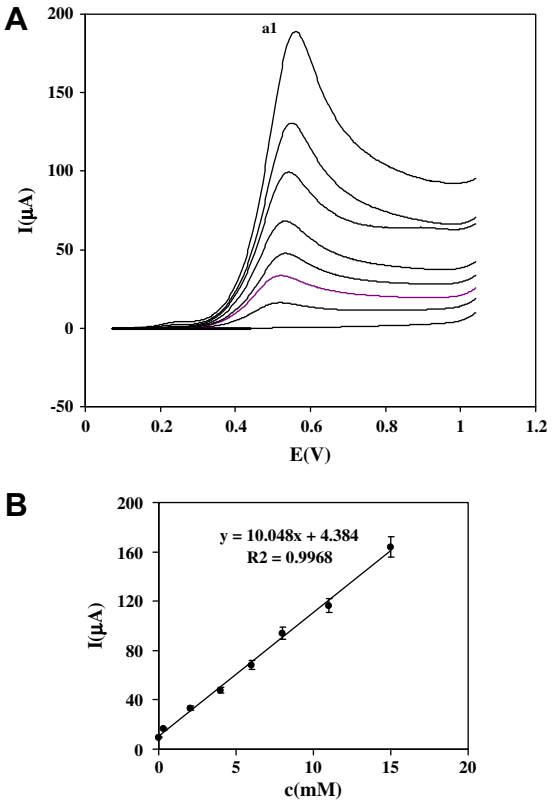

Fig. 7. (A) DPVs obtained for determination of Cys in 100 mM NaOH. Cys concentrations (from inner to outer) are 0.01, 0.1, 1, 4, 6, 8, 10, and 15 mM. (B) The related calibration graph for peak a1.

Table 2
Results obtained for Cys analysis from 100 mM NaOH.

10–15,000	Linear range (μM)
0.010048	Slope ($A \cdot M^{-1}$)
4.384×10^{-3}	Intercept (M)
3.40	RSD (%)[a]
4.34	LOD (μM)
8.52	LOQ (μM)

[a] Each value was obtained from 10 experiments.

Table 3
Results obtained for some amino acid from 100 mM NaOH.

RSD (%)	LOQ (μM)	LOD (μM)	Linear range (μM)	Amino acid
3.40	8.52	4.34	10–15,000	Cys
1.30	17.44	10.02	20–1500	Gly
1.05	11.00	5.21	13–6000	Tyr
5.21	9.54	5.31	100–1000	Ser
5.00	18.00	9.86	25–10,000	Val
2.71	7.89	4.44	10–1500	l-Arg
1.44	25.51	13.70	30–2000	l-Phe
3.90	4.22	1.10	3–12,500	l-Trp

acid electrooxidation in alkaline solution. The electrode was electrocatalytically active around 550 mV/SCE where the GC electrode possessed no activity. Chronoamperometric work showed a large anodic current at the oxidation potential of low-valence cobalt hydroxide (oxide) in further support of the mediated electrooxidation. Using cyclic voltammetry and chronoamperometry techniques, the kinetic parameters of these bimolecular reactions, such as the charge transfer coefficient, catalytic reaction rate constant, and diffusion coefficient for oxidation, were determined. The kinetics of the reaction based on the above mechanism was developed, and the magnitudes of the rate constants and anodic transfer coefficient of the electrooxidation reaction were obtained.

Acknowledgments

We gratefully acknowledge the support of this work by Payame Noor University and Arak University of Technology Research Council. Thanks also go to A. James McQuillan (Otago University, New Zealand) for his valuable comments.

References

[1] Y. Xie, S. Dong, Electrooxidation of ascorbic acid at the bis(4-pyridyl)disulfide modified gold electrode, Electroanalysis 6 (1994) 119–123.
[2] B. Nalini, S.S. Narayanan, Amperometric determination of ascorbic acid based on electrocatalytic oxidation using a ruthenium(III) diphenyldithiocarbamate-modified carbon paste electrode, Anal. Chim. Acta 405 (2000) 93–97.
[3] D. Leech, J. Wang, M.R. Shysmth, Electrocatalytic detection of streptomycin and related antibiotics at ruthenium dioxide modified graphite–epoxy composite electrodes, Analyst 115 (1990) 1447–1450.
[4] S. Dong, G.J. Che, Electrocatalysis at a microdisk electrode modified with a redox species, J. Electroanal. Chem. 309 (1991) 103–114.
[5] F.M. Hawkridge, I. Taniguchi, The direct electron transfer reactions of cytochrome *c* at electrode surfaces [comment], Inorg. Chem. 17 (1995) 163–187.
[6] A.S. Praximos, H. Günther, D.J.M. Schoneddings, H. Simon, Direct electron transfer from modified glassy carbon electrodes carrying covalently immobilised mediators to a dissolved viologen accepting pyridine nucleotide oxidoreductase and dihydrolipoamide dehydrogenase, Bioelectrochem. Bioenerg. 25 (1991) 425–436.
[7] A. Nelson, Electroanalysis and chemometrics of speciation of natural waters, Anal. Proc. 28 (1991) 58–72.
[8] J. Wang, T. Golden, Permselectivity and ion-exchange properties of Eastman-AQ polymers on glassy carbon electrodes, Anal. Chem. 61 (1989) 1397–1400.
[9] K-K. Shiu, O.Y. Chan, S-K. Pang, Factors affecting the electroanalytical behavior of polypyrrole-modified electrodes bearing complexing ligands, Anal. Chem. 67 (1995) 2828–2834.
[10] V.E.M. Filho, A.L.B. Marques, J.J. Zhang, G.O. Chierice, Surface complexation of copper(II) with Alizarin Red S adsorbed on a graphite electrode and its possible application in electroanalysis, Electroanalysis 11 (1999) 1130–1136.
[11] N. Chebotareva, T. Nyokong, Metallophthalocyanine catalysed electroreduction of nitrate and nitrite ions in alkaline media, J. Appl. Electrochem. 27 (1997) 975–983.
[12] Y. Lei, F.C. Anson, Dynamics of the coordination equilibria in solutions containing copper(II), copper(I), and 2,9-dimethyl-1,10-phenanthroline and their effect on the reduction of O_2 by Cu(I), Inorg. Chem. 34 (1995) 1083–1093.
[13] X. Qi, R.P. Baldwin, Selective oxidation of thiols to disulfides at polymeric cobalt phthalocyanine chemically modified electrodes, J. Electrochem. Soc. 143 (1996) 1283–1287.
[14] J. Wang, P.V.A. Pamidi, C. Parrade, D.S. Park, Sol–gel-derived cobalt phthalocyanine-dispersed carbon composite electrodes for electrocatalysis and amperometric flow detection, Electroanalysis 9 (1997) 908–911.
[15] S.A. Wring, J.P. Hard, B.J. Birch, Voltammetric behaviour of ascorbic acid at a graphite–epoxy composite electrode chemically modified with cobalt phthalocyanine and its amperometric determination in multivitamin preparations, Anal. Chim. Acta 229 (1990) 63–70.
[16] M.E.G. Lyons, C.A. Fitzgerald, Glucose oxidation at ruthenium dioxide based electrodes, Analyst 119 (1994) 855–862.
[17] B. Nalini, S.S. Narayanan, Electrocatalytic oxidation of sulfhydryl compounds at ruthenium(III) diphenyldithiocarbamate modified carbon paste electrode, Electroanalysis 10 (1998) 779–783.
[18] E.G. Cookeas, C.E. Efstathiou, Flow injection–pulse amperometric detection of ephedrine at a cobalt phthalocyanine modified carbon paste electrode, Analyst 125 (2000) 1147–1150.
[19] O.A. Petrii, G.A. Tsirlina, Size effects in electrochemistry, Russ. Chem. Rev. 70 (2001) 285–296.
[20] G.C. Silva, C.S. Fugivara, T. Tremiliosi, G. Filho, P.T.A. Sumodjo, A.V. Benedetti, Electrochemical behavior of cobalt oxide coatings on cold-rolled steel in alkaline sodium sulfate, Electrochim. Acta 47 (2002) 1875–1883.
[21] P. Nkeng, J.F. Koening, J.L. Gautier, P. Chartier, G. Poillerat, Enhancement of surface areas of Co_3O_4 and $NiCo_2O_4$ electrocatalysts prepared by spray pyrolysis, J. Electroanal. Chem. 402 (1996) 81–89.
[22] Y. Zhu, H. Li, Y. Koltypin, A. Gedanken, Preparation of nanosized cobalt hydroxides and oxyhydroxide assisted by sonication, J. Mater. Chem. 12 (2002) 729–740.
[23] L.C. Schumacher, I.B. Holzhueter, I.R. Hill, M.J. Dignam, Semiconducting electrocatalytic properties of sputtered cobalt oxide films, Electrochim. Acta 35 (1990) 975–984.
[24] K. Nakaoka, M. Nakayama, K. Ogura, Electrochemical deposition of spinel-type cobalt oxide from alkaline solution of Co^{2+} with glycine, J. Electrochem. Soc. C 149 (2002) 159–165.

[25] M. Houshmand, A. Jabbari, H. Heli, M. Hajjizadeh, A.A. Moosavi-Movahedi, Electrocatalytic oxidation of aspirin and acetaminophen on a cobalt hydroxide nanoparticles modified glassy carbon electrode, J. Solid State Electrochem. 12 (2008) 1117–1128.
[26] I.G. Casella, Electrodeposition of cobalt oxide films from carbonate solutions containing Co(II) tartrate complexes, J. Electroanal. Chem. 520 (2002) 119–125.
[27] K. Ogura, M. Kobayashi, M. Nakayama, Y. Miho, Electrochemical and in situ FTIR studies on the adsorption and oxidation of glycine and lysine in alkaline medium, J. Electroanal. Chem. 449 (1998) 101–109.
[28] S.M. MacDonald, S.G. Roscoe, Electrochemical oxidation reactions of tyrosine, tryptophan, and related dipeptides, Electrochim. Acta 42 (1997) 1189–1200.
[29] D.G. Marangoni, I.G.N. Wylie, S.G. Roscoe, Surface electrochemistry of the oxidation reactions of α- and β-alanine at a platinum electrode, Bioelectrochem. Bioenerg. 25 (1991) 269–284.
[30] Y.S. Fung, S.Y. Mo, Determination of amino acids and proteins by dual-electrode detection in a flow system, Anal. Chem. 67 (1995) 1121–1124.
[31] M. Hasanzadeh, G. Karimnezhad, M.G. Mahjani, M. Jafarian, N. Shadjou, B. Khalilzadeh, L.A. Saghatforoush, A study of the electrocatalytic oxidation of cyclohexanol on copper electrode, Catal. Commun. 10 (2008) 295–299.
[32] M. Hajjizadeh, A. Jabbari, H. Heli, A. Shafiee, K. Karimian, Electrocatalytic oxidation and determination of deferasirox and deferiprone on a nickel oxyhydroxide-modified electrode, Anal. Biochem. 373 (2008) 337–348.
[33] M. Hajjizadeh, A. Jabbari, H. Heli, A.A. Moosavi-Movahedi, S. Haghgoo, Electrocatalytic oxidation of some anti-inflammatory drugs on a nickel hydroxide-modified nickel electrode, Electrochim. Acta 53 (2007) 1766–1774.
[34] H. Heli, A. Jabbari, M. Hajjizadeh, A.A. Moosavi-Movahedi, Copper nanoparticles-modified carbon paste transducer as a biosensor for determination of acetylcholine, Biosens. Bioelectron., in press, doi:10.1016/j.bios.2008.10.036.
[35] A. Babaei, M. Zendehde, B. Khalilzadeh, A. Taheri, Simultaneous determination of tryptophan, uric acid, and ascorbic acid at iron(III) doped zeolite modified carbon paste electrode, Colloids Surf. B 66 (2008) 226–232.
[36] S. Majdi, A. Jabbari, H. Heli, A study of the electrocatalytic oxidation of aspirin on a nickel hydroxide-modified nickel electrode, J. Solid State Electrochem. 11 (2007) 601–607.
[37] S. Majdi, A. Jabbari, H. Heli, A.A. Moosavi-Movahedi, Electrocatalytic oxidation of some amino acids on a nickel–curcumin complex modified glassy carbon electrode, Electrochim. Acta 52 (2007) 4622–4629.
[38] H. Heli, A.A. Moosavi-Movahedi, A. Jabbari, F. Ahmad, An electrochemical study of safranin O binding to DNA at the surface, J. Solid State Electrochem. 11 (2007) 593–599.
[39] H. Heli, N. Sattarahmady, A. Jabbari, A.A. Moosavi-Movahedi, G.H. Hakimelahi, F-Y. Tsai, Adsorption of human serum albumin onto glassy carbon surface—applied to albumin-modified electrode: mode of protein–ligand interactions, J. Electroanal. Chem. 610 (2007) 67–74.
[40] C. Barbero, G.A.S. Plane, M.C. Miras, Redox coupled ion exchange in cobalt oxide films, Electrochem. Commun. 3 (2001) 113–119.
[41] P.J. Vandeberg, D.C. Johnson, Pulsed electrochemical detection of cysteine, cystine, methionine, and glutathione at gold electrodes following their separation by liquid chromatography, Anal. Chem. 65 (1993) 2713–2718.
[42] J.C. Hoekstra, D.C. Johnson, Comparison of potential–time waveforms for the detection of biogenic amines in complex mixtures following their separation by liquid chromatography, Anal. Chem. 70 (1998) 83–88.
[43] L.E. Welch, W.R. La Course, D.A. Mead, D.C. Johnson, T. Hu, Comparison of pulsed coulometric detection and potential-sweep-pulsed coulometric detection for underivatized amino acids in liquid chromatography, Anal. Chem. 61 (1989) 555–559.
[44] A.J. Tudos, D.C. Johnson, Dissolution of gold electrodes in alkaline media containing cysteine, Anal. Chem. 67 (1995) 557–560.
[45] D.S. Austin, D.C. Johnson, T.G. Hines, E.T. Berti, Square-wave hydrodynamically modulated voltammetry for study of anodic electrocatalysis, Anal. Chem. 55 (1983) 2222–2226.
[46] S. Bruckenstein, M. Shay, Potential dependence of lead and silver underpotential coverages in acetonitrile using a piezoelectric crystal oscillator method, Electrochim. Acta 30 (1985) 851.
[47] A.J. Bard, L.R. Faulkner, Electrochemical Methods, John Wiley, New York, 2001. p. 503.
[48] J.A. Harrison, Z.A. Khan, The oxidation of hydrazine on platinum in acid solution, J. Electroanal. Chem. 28 (1970) 131–138.
[49] J.C. Miller, J.N. Miller, Statistics for Analytical Chemistry, fourth ed., Ellis Harwood, New York, 1994.